Absolute partial and total cross sections for electron-impact ionization of argon from threshold to 1000 eV

H. C. Straub, P. Renault, B. G. Lindsay, K. A. Smith, and R. F. Stebbings
Department of Physics, Department of Space Physics and Astronomy, and Rice Quantum Institute, Rice University, Post Office Box 1892, Houston, Texas 77251
(Received 21 February 1995)

Absolute partial cross sections from threshold to 1000 eV are reported for the production of Ar^{n+} ($n=1-4$) by electron-impact ionization of argon. The total cross sections, obtained from an appropriately weighted sum of the partial cross sections, are also reported. These results are obtained with an apparatus incorporating a time-of-flight mass spectrometer with position-sensitive detection of the product ions. The simple apparatus design embodies recent developments in pressure measurement and particle detection and is believed to yield more reliable results than those previously reported. For singly charged ions, the overall uncertainty in the absolute cross section values reported here is $\pm 3.5\%$. Previous measurements of absolute partial and total cross sections are reviewed and compared with the present results.

PACS number(s): 34.80.Dp

I. INTRODUCTION

Ionization of atoms and molecules by electron impact is of fundamental importance in atmospheric science, plasma processes, and mass spectrometry. Electron-impact ionization has been investigated experimentally for more than 60 years since the first cross-section measurements [1–4]. Comprehensive reviews [5–8] reveal large discrepancies in both the magnitude and the energy dependences of cross sections reported by different groups. In many instances, limitations of the available instruments such as pressure gauges, mass spectrometers, and particle detectors compromised the accuracy of the early measurements.

Recent developments in instrumentation coupled with the continuing need for accurate cross-section data justify a further study of electron-impact ionization and this paper is the first of a series in which absolute cross sections for some commonly encountered atoms and molecules will be reported. Here we report absolute partial cross sections for the production of Ar^{n+} ($n=1-4$) together with the total cross sections from threshold to 1000 eV. Argon was selected for the initial study because it had previously been studied quite extensively. It should be noted, however, that the principal benefits of the apparatus and technique described here will be fully realized only in the study of molecules where total collection and mass identification of all energetic fragment ions are readily demonstrated.

II. APPARATUS AND EXPERIMENTAL METHOD

The apparatus is shown schematically in Fig. 1. It is contained within a stainless-steel vacuum chamber evacuated by a 6-in. oil diffusion pump to a normal base pressure in the vicinity of 1×10^{-7} Torr. During cross-section measurements, the entire chamber is filled with argon at a pressure of approximately 3×10^{-6} Torr. Pulses of electrons are directed through an interaction region located between two gold-plated copper plates, maintained at ground potential, and then collected in a Faraday cup. Following each electron pulse, an electric field applied briefly across the interaction region drives the positive ions formed by electron impact toward the bottom plate. Some of these ions pass through an aperture in this plate, which is covered with an electroformed grid, and impact a position-sensitive detector (PSD) that records both their arrival times and positions. The apparatus is interfaced through computer automated measurement and control to a laboratory computer that controls the experiment and records the data.

Under conditions in which very few of the incident electrons produce an ion, the partial cross section σ^{n+} for production of Ar^{n+} is given by

$$\sigma^{n+}=\frac{N_i^{n+}}{N_e n l}\ , \tag{1}$$

where N_i^{n+} is the number of Ar^{n+} produced by a number N_e of electrons passing a distance l through a uniform argon gas target of density n. The essence of the present experiment is accurate measurement of the quantities appearing on the right-hand side of this equation.

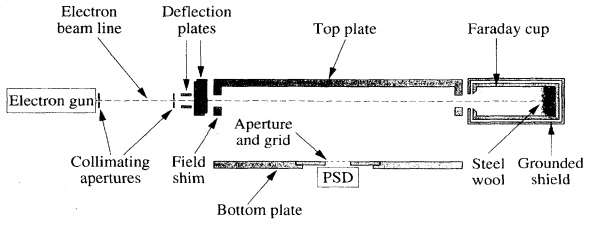

FIG. 1. Schematic diagram of the apparatus.

1050-2947/95/52(2)/1115(10)/$06.00

A. Measurement of N_e

The electron beam is generated by a television tube gun [9] in which the electrons are emitted from an indirectly heated oxide-coated cathode and pass through an electrostatic lens assembly. The first lens element, which has a small aperture, is the control grid of the gun. It is normally biased to cut off the electron flow, but is pulsed at 2.5 kHz with 20-ns positive pulses, producing a pulsed electron beam. Collimation is achieved by two 760-μm-diam gold-plated copper apertures separated by 5.65 cm and held in place by a gold-plated copper support cylinder. Each beam pulse emerging from the second aperture contains about 2500 electrons that pass through two sets of gold-plated copper deflection plates, travel approximately 20 cm through the interaction region, and ultimately enter the Faraday cup. The electron beam axis lies 1.2 cm below the top plate, which is separated from the bottom plate by 6.2 cm. The beam diverges slowly as it passes through the interaction region, having a diameter of approximately 4 mm when it is over the center of the PSD and 7 mm when it enters the Faraday cup. The beam current is measured by a Cary model 401 vibrating reed electrometer operating in the charge collection mode. The beam energy is established to better than ± 1 eV by observing the threshold for He^+ formation. Since the current produced by the electron gun decreases rapidly below 20 eV, using the relatively high threshold for He^+ formation (~ 24.6 eV) allows the electron energy calibration to be performed more accurately.

Prior to taking cross-section data, the electron beam is swept across the entrance to the Faraday cup to determine the correct operating voltages for the deflection plates and to ensure that the entire beam always enters the Faraday cup. The cup is 6 cm deep, with an entrance aperture 1.2 cm in diameter, and is biased 30 V positive with respect to a surrounding grounded shield to prevent the escape of the low-energy secondary electrons. This bias results in a leakage current of approximately 10^{-14} A. This current is frequently checked and results in a correction of approximately 1% to the measured electron current since the averaged dc Faraday cup current is typically 10^{-12} A. Escape of reflected high-energy electrons is limited by the small solid angle subtended at the bottom of the cup by the entrance aperture and further reduced by covering the bottom of the cup with steel wool. A high-permeability magnetic shield encloses the apparatus reducing the ambient magnetic field to approximately 30 mG so that the trajectories of the primary electrons are essentially linear.

B. Measurement of N_i^{n+}

Collisions of electrons with argon lead to the production of both singly and multiply charged ions. Approximately 200 ns after each electron pulse, a 2-kV voltage pulse, with a 300-ns rise time, is applied to the top plate of the interaction region and two-thirds of this voltage is simultaneously applied to the field shims at the ends of the interaction region. This extraction pulse accelerates positive ions formed by electron impact toward the PSD. An additional 3-kV bias between the bottom plate gird and the front of the PSD results in an impact energy on the detector of approximately 4.6 keV for singly charged ions. The PSD comprises a pair of 25-mm-diam microchannel plate electron multipliers located in front of a resistive encoded anode [10]. The PSD output provides the ion-impact positions to a nominal accuracy of ± 50 μm and the ion arrival times to within ± 1 ns [11].

The ions are identified from their measured flight times, which are given by the delay between initiation of the extraction pulse and the ion arrival times at the detector. Figure 2 shows a typical time-of-flight spectrum exhibiting a number of well-resolved peaks. The total count rate is typically about 200 Hz at the Ar^+ cross-section maximum. Both the position and time of arrival of each ion are recorded, although only the time information is used for computing cross sections. The background ion signal is found by removing all argon from the chamber and observing the time-of-flight spectrum. The background correction to all of the observed signals is less than 1%. The data-acquisition electronics allow only one ion to be detected following each electron pulse. Occasionally, more than one ion is created during an electron pulse and a small dead-time correction, which is discussed in the Appendix, is applied to compensate for missed counts.

Determination of N_i^{n+} for the different ions requires knowledge of the detection efficiency for each ion species. To accomplish this, a weak ($\sim 10^4$ particles per second) ion beam of the appropriate species and energy is directed through an aperture in the top plate of the interaction region, which is opened solely for this purpose. This ion beam [12] is repetitively positioned alternately on the PSD and in a Faraday cup (not shown in Fig. 1). The detection efficiencies are then determined by comparing the number of timing output pulses from the PSD with the charge accumulated by the Faraday cup. The ion-beam current in the Faraday cup is measured using the same Cary model 401 electrometer used to measure the electron beam current. The efficiencies are found to have

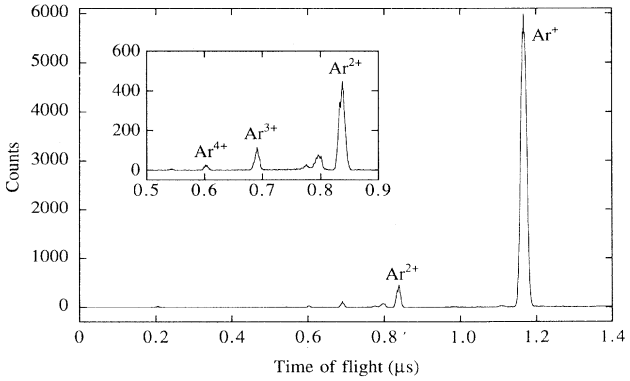

FIG. 2. Time-of-flight spectrum for Ar^{n+} ions produced by 1000-eV electrons. The peaks seen at approximately 0.8 μs are due to water vapor, the principal background gas present in the vacuum system. The widths of the argon ion peaks are primarily due to the spatial extent of the electron beam.

values between 40.0% and 40.5% for all ions, irrespective of their charge. When account is taken of the fact that, in transit to the PSD, the ions pass through the electroformed grid [13] of 65% transparency, it is seen that the detection efficiency of the PSD itself is 62%, which is equal to the percentage of the area of the first microchannel plate that is occupied by the channel openings [14]. Thus, regardless of its charge, every argon ion that enters a microchannel is detected with unit efficiency. In addition to these measurements of the efficiency, the PSD's spatial uniformity is determined by repetitively placing the calibration ion beam at 35 different positions on the PSD face and measuring the relative detection efficiency at each location. These measurements reveal a spatial uniformity of better than $\pm 2\%$. In that the same electrometer is used for determination of N_e and for calibration of the ion detector, reference to Eq. (1) shows that any calibration error of the electrometer itself should not affect the final cross-section measurements. Nonetheless, the electrometer was subjected to regular calibration checks.

Figure 3 gives a typical ion arrival distribution at the PSD indicating that all ions are detected in a narrow strip centered under the electron beam. The working pressure of 3×10^{-6} Torr is sufficiently low that negligible loss of product ions by charge exchange occurs in transit to the detector.

C. Measurement of l

Ions are created along the entire length of the electron beam and it is therefore essential to identify the path length l from which the detected ions originate. The electron beam passes directly above the center of the 25-mm-diam PSD while traveling through the interaction region. A copper mask placed immediately in front of the PSD has a rectangular aperture (2.54 cm normal to the electron beam direction by 1.91 cm in the parallel direction) covered with an electroformed copper grid. The top and bottom plate electrodes defining the interaction region are large (19 cm in the direction parallel to the electron beam by 15 cm in the perpendicular direction) compared to the dimensions of the PSD in order to minimize extraction field nonuniformities.

If the pulsed extraction field accelerates ions only in a direction normal to the plate electrodes, ions with no initial velocity that pass through the rectangular aperture in the bottom plate and impact the PSD must have originated from a region directly above the aperture whose length is identical to the 1.91 cm length of the aperture. The argon ions, however, do have a small initial velocity due to their thermal energy. Ions produced in the region directly above the edge of the aperture may travel parallel to the electron beam and escape detection. However, the translational symmetry of the apparatus along the electron-beam axis and the extraction field uniformity together ensure that for every ion produced over the PSD that is not detected, one from outside this region is detected. Therefore, the length from which ions are collected is accurately given by the aperture dimension in the direction parallel to the electron beam.

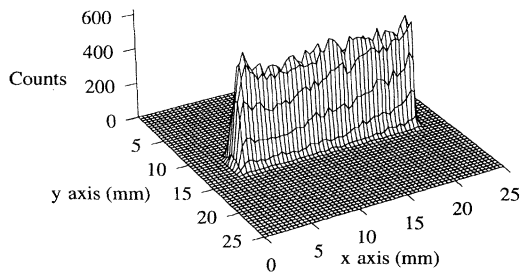

FIG. 3. Arrival position data for Ar^+ ions produced by 1000-eV electrons.

Computer modeling with the program SIMION [15] confirms that with this electrode structure the electric field in the volume of interest above the detector is highly uniform and perpendicular to the plate faces. Modeling also showed that the field shims shown in Fig. 1 further ensure that the electric field is particularly uniform near the top plate where the ions have low velocities and are most sensitive to nonuniformities in the extraction field.

As further confirmation of the extraction field's uniformity, the Faraday cup is temporarily replaced with one having several apertures at known locations in the plane parallel to the plates. The electron beam is then deflected to enter each of these apertures in turn and the corresponding ion arrival positions at the PSD are recorded. Since the geometries of the deflection plates, the interaction region, and the multiaperture cup are known, the precise location of the electron beam above the PSD during each of these measurements can be established. The position data from the detector then confirm that the acceleration of the ions is always highly perpendicular to the plates, demonstrating that l is given accurately by the dimension of the aperture parallel to the electron beam to better than $\pm 1\%$.

D. Measurement of n

The vacuum chamber is filled with approximately 3×10^{-6} Torr of argon and the pressure is measured by a capacitance diaphragm gauge [16]. This gauge is maintained at a temperature of 45 °C while the apparatus temperature is 28 °C (as measured by a thermocouple affixed to the bottom interaction region plate). The pressure recorded by the gauge must therefore be reduced by 2.8% to account for the effects of thermal transpiration [17]. By computer averaging 500 000 readings of the gauge's output, the pressure is determined with a statistical uncertainty of $\pm10^{-7}$ Torr in addition to a systematic uncertainty of $\pm 1\%$ associated with the demonstration of the gauge's linearity down to 10^{-6} Torr [18]. The number density n is obtained from the pressure p_g measured by the capacitance diaphragm gauge using thermal transpiration and the ideal gas law such that

$$n=\frac{p_g}{k\sqrt{T_g T_a}}\ , \tag{2}$$

where k is Boltzmann's constant and T_g and T_a are the

temperatures of the capacitance diaphragm gauge and the apparatus, respectively.

The argon used in this work was obtained from Matheson Gas Products and has a minimum specified purity of 99.998%. It is transported from its container through stainless-steel tubing and introduced to the vacuum chamber through a leak valve. The effectiveness of these procedures in preventing contamination of the argon can be seen from the absence of spurious peaks in the time-of-flight spectrum.

E. Measurement of cross sections

Since the procedure for absolute cross-section measurements is complex, the cross sections reported here are determined in a two-step procedure whereby the relative cross sections are first obtained as a function of electron energy and then made absolute by normalizing to the absolute cross sections measured at 200 eV.

Due to difficulties operating the electron gun over a wide energy range during a given run, the relative cross sections are measured over a limited range on any given day. The energy ranges are chosen so that they overlapped at 50, 90, 200, and 500 eV and could therefore be normalized relative to one another in order to produce relative cross sections from threshold to 1000 eV. The procedure for measuring the relative partial cross sections, over any one of these ranges, entails recording the time-of-flight spectrum and integrated electron-beam charge alternately at the reference energy and at one of a series of other energies within the range. From the recorded data, the ratios N_i^+/N_e and N_i^{n+}/N_i^+ are determined. The reference energy N_i^+/N_e ratios are used to correct for slow drifts in the argon pressure, which are typically about 5% during the course of a day. The corrected N_i^+/N_e ratios then provide the relative single-ionization cross sections. At each energy, the product of the relative single-ionization cross sections and the N_i^{n+}/N_i^+ ratios then provides the relative multiple-ionization cross sections. Each individual measurement typically takes about 15 min; however, to improve the counting statistics, additional time is spent determining N_i^{n+}/N_i^+ for $n=3,4$.

Subsequently, measurements of the absolute cross sections are carried out at 200 eV by recording the time-of-flight spectrum and the integrated electron-beam charge while measuring the argon pressure. These measurements are more complex because the argon pressure determination entails frequent checks of the capacitance diaphragm gauge zero to compensate for zero drift of the gauge. The zero drifts are typically 2×10^{-8} Torr/min, but repetitive measurements of the zero (every 2.5 min) allow one to assess the argon pressure with a statistical uncertainty of $\pm2.5\%$ at 3×10^{-6} Torr.

Figures 4 and 5 show that the measured Ar^+ cross section is independent of electron-beam current and argon pressure, respectively. As a consistency check, additional measurements of the absolute value of the cross section at five energies other than 200 eV were made and found to agree with the normalized relative cross sections to within the uncertainties stated in the following subsection. The absolute cross section for Ar^+ at 200 eV was measured with the capacitance diaphragm gauge sampling the argon pressure inside and then outside the high-permeability magnetic shield that encloses the apparatus. The measured cross section was the same each time, indicating that significant pressure gradients were not present.

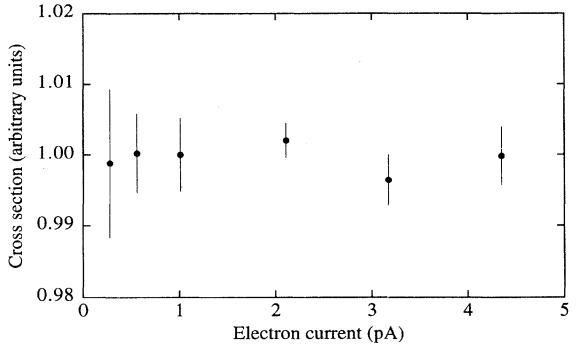

FIG. 4. Measured cross sections for production of Ar^+ as a function of the averaged dc electron-beam current at an electron energy of 200 eV. A current of 1 pA corresponds to approximately 2500 electrons per pulse, the typical operating condition used during cross section measurements.

F. Measurement uncertainties

Table I shows the uncertainties in the measured relative and absolute cross sections. The uncertainties in the relative cross sections come primarily from the counting statistics for each species and the uncertainty in determining the number of electrons. One standard deviation in the counting statistics for Ar^+, Ar^{2+}, Ar^{3+}, and Ar^{4+} is $\pm0.5\%$, $\pm2\%$, $\pm3.5\%$, and $\pm7.5\%$, respectively, except near thresholds. The relative uncertainty in the elec-

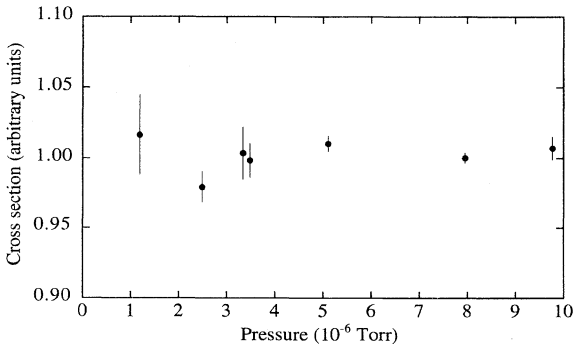

FIG. 5. Measured cross sections for production of Ar^+ as a function of argon pressure at an electron energy of 200 eV. The weighted sum of the data on an absolute scale is 2.18×10^{-16} cm^2. The independence of the measured cross section with respect to the argon pressure demonstrates that loss of ions from charge exchange is negligible in the present experiment.

TABLE I. Uncertainties associated with the various cross sections. The uncertainties for σ^{total} come from an appropriately weighted sum of the uncertainties for the partial cross sections.

Cross section	Relative uncertainty (%)	Absolute uncertainty at 200 eV (%)	Absolute uncertainty at all other energies (%)
σ^{+}	±2	±3	±3.5
σ^{2+}	±3	±3.5	±4.5
σ^{3+}	±4	±4.5	±6
σ^{4+}	±8	±8	±11
σ^{total}	±2	±3	±3.5

TABLE II. Results for the partial and total cross sections of argon.

Energy (eV)	σ^{+} (10^{-16} cm^2)	σ^{2+} (10^{-17} cm^2)	σ^{3+} (10^{-19} cm^2)	σ^{4+} (10^{-19} cm^2)	σ^{total} (10^{-16} cm^2)
17	0.017				0.017
20	0.46				0.46
25	1.24				1.24
30	1.84				1.84
35	2.26				2.26
40	2.55				2.55
45	2.66	0.0048			2.66
50	2.70	0.128			2.73
55	2.69	0.418			2.77
60	2.67	0.856			2.84
65	2.67	1.21			2.91
70	2.67	1.46			2.96
75	2.66	1.56			2.97
80	2.69	1.70			3.03
85	2.70	1.79			3.06
90	2.69	1.84			3.06
95	2.67	1.90	0.51		3.05
100	2.64	1.89	1.03		3.02
110	2.61	1.91	2.21		3.00
120	2.55	1.87	3.23		2.93
140	2.45	1.77	4.94		2.81
160	2.35	1.65	5.57		2.70
180	2.27	1.58	5.68		2.60
200	2.18	1.44	5.53		2.49
225	2.10	1.31	5.30		2.37
250	1.99	1.25	5.23		2.25
275	1.87	1.13	5.09		2.11
300	1.79	1.08	5.03		2.02
350	1.63	0.953	5.99	0.17	1.84
400	1.51	0.872	6.32	0.44	1.71
450	1.39	0.759	6.50	0.77	1.57
500	1.31	0.679	6.97	1.07	1.47
550	1.23	0.623	7.08	1.18	1.38
600	1.16	0.575	7.41	1.32	1.30
650	1.09	0.552	7.19	1.27	1.23
700	1.03	0.524	7.23	1.33	1.16
750	0.976	0.496	6.97	1.42	1.10
800	0.932	0.456	6.96	1.50	1.05
850	0.901	0.425	7.09	1.42	1.01
900	0.865	0.419	6.51	1.33	0.973
950	0.824	0.394	6.51	1.36	0.927
1000	0.795	0.374	6.57	1.32	0.895

trometer reading is ±0.5%, caused predominately by fluctuations in the background electrometer signal. The uncertainty for the relative single-ionization cross sections comes from the root-mean-square sum of the measurement uncertainties at the reference energies and other energies. The uncertainties in the relative multiple-ionization cross sections are then determined by the root-mean-square sum of the statistical uncertainties for the appropriate ion together with those for the relative single-ionization cross sections.

Absolute cross sections at the reference energy are determined by measuring each of the quantities in Eq. (1). Since the number of ions is determined from the product of the number of counts of the appropriate species and the detection efficiency, the uncertainty in the number of ions is given by the appropriate counting statistics together with the ±0.5% relative uncertainty in the determination of the detection efficiency due to the electrometer. The relative uncertainty in the measurement of electrons is again ±0.5%. As discussed previously, the same electrometer is used for determining the detection efficiency of ions and measuring the number of electrons. By use of a current source [19], it was verified that the electrometer calibration is independent of both the sign of the charge measured and its magnitude to within ±0.5%. The pressure measurement uncertainty consists of a ±2.5% statistical uncertainty and a ±1% calibration uncertainty. The temperature measurements required for computation of the number density each contribute ±0.2% to the uncertainty of the absolute cross section. Finally, the uncertainty in the target length is ±1%. Since the absolute cross sections reported here are obtained by normalizing the relative cross sections to the absolute cross section measured at 200 eV, the uncertainties in the absolute cross sections at energies other than 200 eV are obtained from a root-mean-square sum of the relative cross section uncertainties and the 200-eV absolute cross section uncertainties given in Table I.

III. RESULTS AND DISCUSSION

Table II gives the measured partial cross sections for Ar^{n+} with $n=1-4$. These data are also plotted in Figs. 6–9 together with previously published absolute partial cross sections. Not shown are relative cross-section measurements [20–25] that were normalized to the work of others, most commonly that of Rapp and Englander-Golden [26].

The total cross sections, which are the weighted sum of the partial cross sections, are

$$\sigma^{\text{total}}=\sigma^{+}+2\sigma^{2+}+3\sigma^{3+}+4\sigma^{4+}+\cdots \tag{3}$$

and are given in Table II and shown in Fig. 10 together with previously published direct measurements of σ^{total}. Since Figs. 6–10 reveal considerable variation in the cross-section values and energy dependences, we have examined the literature in an attempt to assemble a coherent picture of earlier measurements and to identify possible sources of error.

Earlier cross-section measurements were carried out using argon both as a static gas target and as a neutral beam. In the former arrangement, the electron beam, either dc or pulsed, traversed an interaction region containing argon at a measured pressure. Some experiments measured the total positive charge produced to determine total cross sections, while others extracted the ions and mass analyzed them to determine partial cross sections. The crossed-beam experiments were carried out using both effusively produced thermal energy beams and fast beams produced by charge transfer of keV energy Ar^{+} ions. However, it is only possible to determine the beam overlap function [27] and thus the absolute cross sections in the case of fast beams.

Although each of these experimental methods has its own unique set of problems, it is reasonable to assert that the approach employing a static gas target gas, a dc elec-

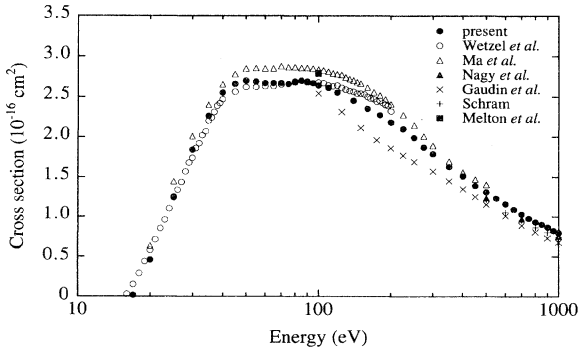

FIG. 6. Present Ar^{+} cross sections together with the results of Wetzel *et al.* [36]; Ma, Sporleder, and Bonham [33]; Nagy, Skutlartz, and Schmidt [29]; Gaudin and Hagemann [28]; Schram [30]; and Melton and Rudolph [32].

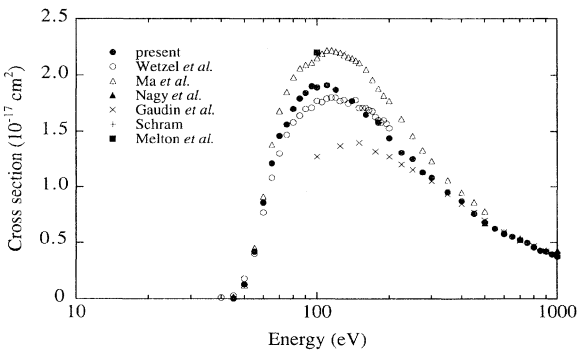

FIG. 7. Present Ar^{2+} cross sections together with the results of Wetzel *et al.* [36]; Ma, Sporleder, and Bonham [33]; Nagy, Skutlarz, and Schmidt [29]; Gaudin and Hagemann [28]; Schram [30]; and Melton and Rudolph [32].

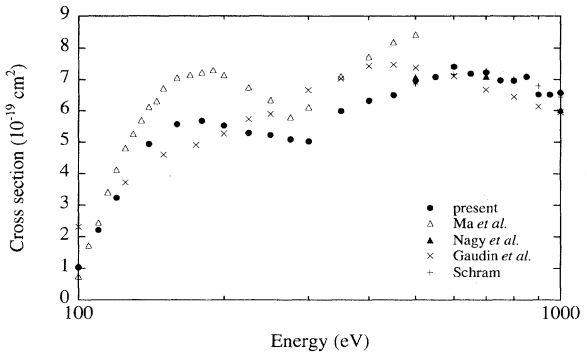

FIG. 8. Present Ar^{3+} cross sections together with the results of Ma, Sporleder, and Bonham [33]; Nagy, Skutlartz, and Schmidt [29]; Gaudin and Hagemann [28]; and Schram [30].

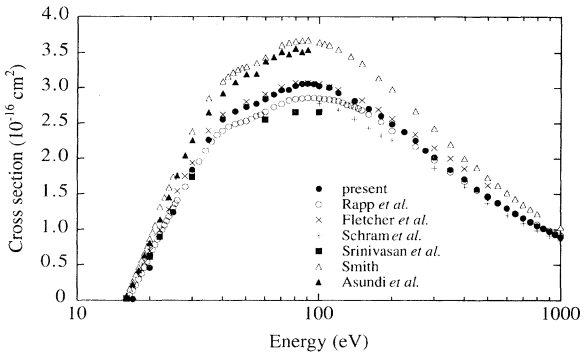

FIG. 10. Present total cross sections together with the results of Rapp and Englander-Golden [26]; Fletcher and Cowling [37]; Schram *et al.* [31,39]; Srinivasan and Rees [40]; Smith [3]; and Asundi and Kurepa [38].

tron beam, and total charge collection is inherently the simplest and most likely to yield accurate results. However, this approach leads only to a determination of the total cross sections. To obtain partial cross sections, some form of mass spectrometry, which adds complexity to the experiment, is required. The relevant features of the various absolute experiments are discussed below.

A. Partial cross sections

In the work of Gaudin and Hagemann [28], a dc electron beam was passed through a static gas and the resulting ions were extracted, separated with a magnetic field sector analyzer, and detected with a calibrated electron multiplier. A Bayard-Alpert ionization gauge calibrated against a McLeod gauge gave the target gas density. Nagy, Skutlartz, and Schmidt [29] used a similar method to measure absolute partial cross sections and furthermore addressed the issues of ion transport and detection efficiency. They also used an ionization gauge, but determined its calibration with a capacitance diaphragm gauge. In the work of Schram [30] an apparatus similar to that of Gaudin and Hagemann produced relative partial cross sections, which were then normalized to total cross sections [31] also measured by them with a parallel plate apparatus. For the total cross-section measurements, a McLeod gauge, corrected for mercury pumping errors, provided pressure measurements. Thus, in none of these experiments was the target gas number density determined directly using a reliable absolute pressure gauge. Furthermore, they all faced the complexities involved in transporting ions over quite long distances throughout which the target gas was present. Melton and Rudolph [32] also used a technique similar to that of Gaudin and Hagemann including a calibrated ionization gauge; however, they differentially pumped the magnetic-field sector analyzer to avoid transporting the ions long distances through the target gas.

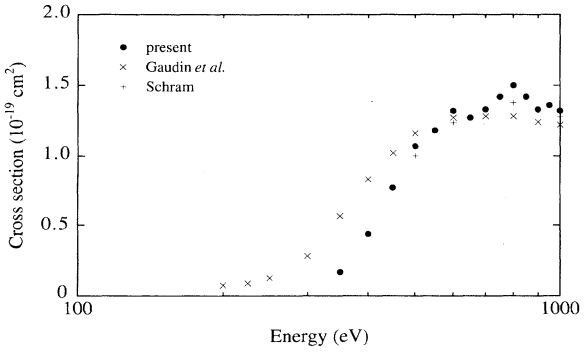

FIG. 9. Present Ar^{4+} cross sections together with the results of Gaudin and Hagemann [28] and Schram [30].

A time-of-flight mass spectrometer was used in the recent work of Ma, Sporleder, and Bonham [33]. A spinning rotor gauge, calibrated by a capacitance diaphragm gauge, was used to measure the argon pressure while a pair of microchannel plates was utilized for ion detection. The path length from which ions were collected was not directly measured but was instead determined through computer modeling. Subsequent work [34] led to an upward revision of 15% in the Ar^+ cross section to account for ion detection efficiency problems and loss of ions in transport through the target gas to the detector. Since Ma, Sporleder, and Bonham state an uncertainty of $\pm 15\%$, their results are not inconsistent with the present results, although they typically lie 5–10% higher than the present results.

The crossed-beam technique employed by Peterson [35] and more recently by Wetzel *et al.* [36] using fast neutral beam targets has the advantage that the collection and mass analysis of the product ions is relatively straightforward because of the directed motion of the target particles prior to ionization. However, an accurate absolute measurement of the overlap integral presents formidable difficulties. Furthermore, the possibility that Rydberg and other long-lived atoms are present in the

neutral beam [27] raises some doubt regarding its purity. Nevertheless, the recent work of Wetzel *et al.* agrees quite closely in absolute magnitude with the present results but falls more slowly with increasing energy. The earlier results of Peterson exhibit neither the absolute magnitude nor the energy dependence of any of the other results and are not shown in Figs. 6 and 7.

B. Total cross sections

Some experiments measured the total cross section given in Eq. (3) by collection of the total positive charge produced as an electron beam traversed a known length of a gas at a measured pressure. This approach was used very successfully by Rapp and Englander-Golden [26] whose results have become the *de facto* standard. Almost a decade after Rapp and Englander-Golden's work was published, Fletcher and Cowling [37] used a similar apparatus and measured total cross sections that exhibited the same energy dependence as those of Rapp and Englander-Golden but were approximately 7% higher. Rapp and Englander-Golden gave the uncertainty of the energy dependence of their cross sections as $\pm 1\%$ and the uncertainty of the absolute value of their cross sections for argon as $\pm 7\%$. The larger uncertainty in the absolute value is mainly due to concerns regarding measurement of the target pressure, which was accomplished using an effusive flow apparatus calibrated with a McLeod gauge. Fletcher and Cowling gave an uncertainty of $\pm 4.5\%$ for the absolute value of their argon cross sections. Their measurements are thus consistent with those of Rapp and Englander-Golden but may provide better absolute values since their pressures were measured with an ionization gauge calibrated with a capacitance diaphragm gauge.

Total cross sections were also determined using essentially the same technique by Smith [3], Asundi and Kurepa [38], Schram *et al.* [31,39], and Srinivasan and Rees [40]. The early measurements of Smith and Asundi and Kurepa lie 15–20 % higher than the others probably due to their use of McLeod gauges uncorrected for the mercury pumping effect. The remaining work is in general accord with Rapp and Englander-Golden in both absolute magnitude and energy dependence. The most significant source of uncertainty in all of the total cross-section measurements is clearly that associated with the measurement of pressure. The present results are the only ones in which a capacitance diaphragm gauge was used to measure pressure directly during the course of the experiment.

The present results and those of Rapp and Englander-Golden and Fletcher and Cowling agree as to the absolute value of the cross sections to within the combined uncertainties, although they do not agree as to the energy dependence of the cross sections for which an uncertainty of $\pm 2\%$ or less is claimed for all three measurements. Relative to the data of Rapp and Englander-Golden and Fletcher and Cowling, the present results fall too rapidly with increasing energy to be consistent within the stated uncertainties. This is not a large effect, but it is troubling nonetheless.

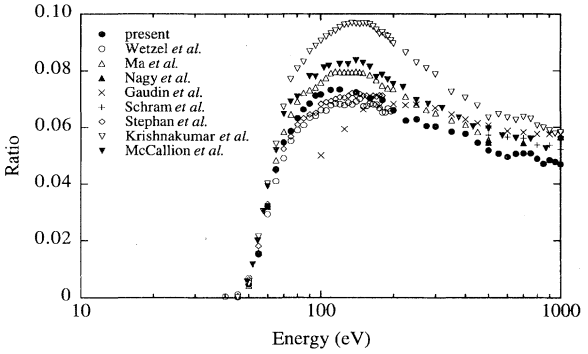

FIG. 11. Present results for the ratios of the cross sections for Ar^{2+} to that for Ar^{+} together with the results of Wetzel *et al.* [36]; Ma, Sporleder, and Bonham [33]; Nagy, Skutlartz, and Schmidt [29]; Gaudin and Hagemann [28]; Schram [30]; Stephan, Helm, and Märk [21]; Krishnakumar and Srivastava [22]; and McCallion, Shah, and Gilbody [24].

C. Cross-section ratios

Even though the ratio of partial cross sections do not provide as much information as absolute partial cross sections, ratios have often been studied since they appear to be easier to determine. Figure 11 shows cross-section ratios obtained from the data in Table II along with the results of some other researchers. In recent articles, Tarnovsky and Becker [25] and Bonham and Bruce [41] noted that the reported ratios generally do not agree to within the stated uncertainties while the absolute partial cross sections often do. This is possibly because absolute partial cross sections are reported with uncertainties as large as $\pm 15\%$ while the uncertainties of ratios are reported as low as $\pm 2\%$ since it is often assumed that systematic effects cancel.

The present work is believed to be an accurate determination of cross-section ratios since possible systematic effects are either eliminated or are explicitly measured. In particular, the detection efficiency for each ion is explicitly measured and the simple geometry of the apparatus ensures that each ion is extracted from the same path length. Since time of flight is used for mass spectrometry, all product ions are measured within the same time interval and any variations in either the electron current or argon pressure will cancel.

IV. CONCLUSION

We describe an apparatus developed to measure absolute partial cross sections for electron-impact ionization of atoms and molecules. The apparatus design is simple and incorporates recent improvements in particle detection and pressure determination, thereby minimizing the possibility of error in the measurement of key experimental parameters. Specifically, accurate measurement of the signals of different product ions is made possible by the very short path length (~ 5 cm) in the time-of-flight mass spectrometer, which ensures a negligible loss of ions either by collisional or trajectory effects while in transit to

the detector. Furthermore, the use of a position-sensitive detector allows the impact positions of the product ions to be observed confirming their complete collection. The ion trajectories are found to be in accordance with those expected on the basis of the electrode and field configuration, thus ensuring that the path length from which ions are collected is well known. Direct measurements of the detection efficiency of the PSD demonstrates that it is the same for each argon ion regardless of charge. Finally, the direct use of an absolute capacitance diaphragm gauge eliminates the uncertainties traditionally associated with measurement of the target gas density. We present data for argon and compare our results with those of earlier experiments.

ACKNOWLEDGMENTS

We gratefully acknowledge support by the Atmospheric Sciences Section of the National Science Foundation and by the Robert A. Welch Foundation. In addition, we have had several useful discussions with B. Van Zyl and R. A. Bonham.

APPENDIX: DEAD-TIME CORRECTION

Since the data-acquisition electronics only allow one ion to be detected following each electron pulse, a correction must be applied to account for pulses in which more than one detectable ion is formed. The correction is computed for specific parts of the time spectrum in which argon peaks occur.

If N_p electron pluses result in the observation of N_b ions before the peak of interest and N_d ions within the peak, then the true number of ions N_d^T in the peak can be computed using the Poisson distribution. The Poisson distribution $P(m,\mu)$ [42] given by

$$P(m,\mu)=\frac{\mu^m}{m!}e^{-\mu} \tag{A1}$$

predicts the probability that m ions are created within the peak where μ is the mean number of ions within the peak per electron pulse (i.e., $\mu=N_d^T/N_p$).

The probability of observing an ion within the peak is the product of the probability that an ion was not observed before the peak and the probability that at least one ion actually occurred within the peak. The probability that an ion was observed before the peak is N_b/N_p, which is one minus the probability that an ion was not observed within the peak. The probability that at least one ion actually occurred within the peak is the sum of the Poisson distribution over m from one to infinity. The number of ions observed within the peak is then given by

$$N_d=N_p\left[1-\frac{N_b}{N_p}\right]\sum_{m=1}^{\infty}P(m,\mu)\ . \tag{A2}$$

The actual number of ions that occur within the peak is found by solving Eq. (A2) for μ and using the definition for μ to compute

$$N_d^T=N_p\ln\left[\frac{N_p-N_b}{N_p-N_b-N_d}\right]\ . \tag{A3}$$

The largest dead time correction ($\sim 8\%$) during the course of the measurements occurs at the cross-section maximum of Ar^+. Figure 4 supports the applicability of Eq. (A3) as it encompasses dead-time corrections ranging from 0.7% to 12%.

[1] A. L. Hughes and E. Klein, Phys. Rev. **23**, 450 (1924).
[2] K. T. Compton and C. C. Van Voorhis, Phys. Rev. **26**, 436 (1925).
[3] P. T. Smith, Phys. Rev. **36**, 1293 (1930).
[4] W. Bleakney, Phys. Rev. **36**, 1303 (1930).
[5] L. J. Kieffer and G. H. Dunn, Rev. Mod. Phys. **38**, 1 (1966).
[6] T. D. Märk, Beitr. Plasmaphys. **22**, 257 (1982).
[7] *Electron Impact Ionization,* edited by T. D. Märk and G. H. Dunn (Springer-Verlag, New York, 1985).
[8] M. A. Lennon *et al.*, J. Phys. Chem. Ref. Data **17**, 1285 (1988).
[9] Model 73Z, Southwest Vacuum Devices, Inc., Tucson, AZ.
[10] Quantar Technology, Inc., Santa Cruz, CA.
[11] R. S. Gao, P. S. Gibner, J. H. Newman, K. A. Smith, and R. F. Stebbings, Rev. Sci. Instrum. **55**, 1756 (1984).
[12] J. H. Newman, K. A. Smith, and R. F. Stebbings, J. Geophys. Res. **90**, 11 045 (1985); R. D. Rundel, D. E. Nitz, K. A. Smith, M. W. Geis, and R. F. Stebbings, Phys. Rev. A **19**, 33 (1979).
[13] Buckbee-Mears, St. Paul, MN.
[14] Varian Electro-Optical Sensors Division, Palo Alto, CA.
[15] D. A. Dahl and J. E. Delmore, SIMION version 5.0 computer program, Idaho National Engineering Laboratory, Idaho Falls, ID, 1991.
[16] Model 690A, 0.1 Torr full scale, MKS Instruments, Inc., Andover, MA.
[17] K. F. Poulter, M. J. Rodgers, P. J. Nash, T. J. Thompson, and M. P. Perkin, Vacuum **33**, 311 (1983).
[18] H. C. Straub, P. Renault, B. G. Lindsay, K. A. Smith, and R. F. Stebbings, Rev. Sci. Instrum. **65**, 3279 (1994).
[19] Model 261, Keithley Instruments, Inc., Cleveland, OH.
[20] M. J. Van der Wiel, T. M. El-Sherbini, and L. Vriens, Physica **42**, 411 (1969).
[21] K. Stephan, H. Helm, and T. D. Märk, J. Chem. Phys. **73**, 3763 (1980).
[22] E. Kishnakumar and S. K. Srivastava, J. Phys. B **21**, 1055 (1988).
[23] J. A. Syage, Chem. Phys. Lett. **143**, 19 (1988); J. Phys. B **24**, L527 (1991).
[24] P. McCallion, M. B. Shah, and H. B. Gilbody, J. Phys. B **25**, 1061 (1992).
[25] V. Tarnovsky and K. Becker, Z. Phys. D **22**, 603 (1992).
[26] D. Rapp and P. Englander-Golden, J. Chem. Phys. **43**, 1464 (1965).
[27] E. W. McDaniel, *Atomic Collisions: Electron and Photon Projectiles* (Wiley, New York, 1989), Chap. 6.
[28] A. Gaudin and R. Hagemann, J. Chim. Phys. **64**, 1209 (1967).

[29] P. Nagy, A. Skutlartz, and V. Schmidt, J. Phys. B **13**, 1249 (1980).
[30] B. L. Schram, Physica **32**, 197 (1966).
[31] B. L. Schram, F. J. De Heer, M. J. Van der Wiel, and J. Kistemaker, Physica **31**, 94 (1965).
[32] C. E. Melton and P. S. Rudolph, J. Chem. Phys. **47**, 1771 (1967).
[33] C. Ma, C. R. Sporleder, and R. A. Bonham, Rev. Sci. Instrum. **62**, 909 (1991).
[34] M. R. Bruce and R. A. Bonham, Z. Phys. D **24**, 149 (1992).
[35] J. R. Peterson, in *Atomic Collision Processes,* Proceedings of the Third International Conference on the Physics of Electronic and Atomic Collisions, London, 1963, edited by M. R. C. McDowell (North-Holland, Amsterdam, 1964), p. 465.
[36] R. C. Wetzel, F. A. Baiocchi, T. R. Hayes, and R. S. Freund, Phys. Rev. A **35**, 559 (1987).
[37] J. Fletcher and I. R. Cowling, J. Phys. B **6**, L258 (1972).
[38] R. K. Asundi and M. V. Kurepa, J. Electron. Control **15**, 41 (1963).
[39] B. L. Schram, H. R. Moustafa, J. Schutten, and F. J. De Heer, Physica **33**, 734 (1966).
[40] V. Srinivasan and J. A. Rees, Br. J. Appl. Phys. **18**, 59 (1967).
[41] R. A. Bonham and M. R. Bruce, Comments At. Mol. Phys. **29**, 19 (1993).
[42] P. R. Bevington, *Data Reduction and Error Analysis for the Physical Sciences* (McGraw-Hill, New York, 1969), Chap. 3.

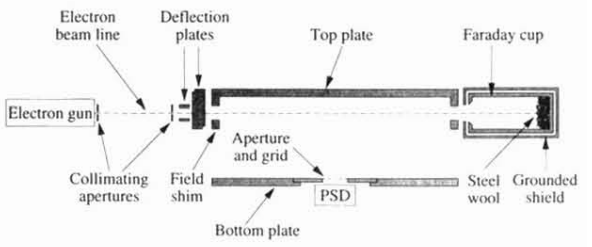

FIG. 1. Schematic diagram of the apparatus.